Radiolarian Biostratigraphy and Faunal Turnover across the Early/Middle Miocene Boundary in the Equatorial Pacific

Authors: Kamikuri, Shin-Ichi, Moore, Theodore C., Matsui, Hiroki, and Nishi, Hiroshi

Source: Paleontological Research, 23(4) : 245-260

Published By: The Palaeontological Society of Japan

URL: https://doi.org/10.2517/2018PR024

Paleontological Research, vol. 23, no. 4, pp. 245–260, October 1, 2019

doi:10.2517/2018PR024

Radiolarian biostratigraphy and faunal turnover across the early/middle Miocene boundary in the equatorial Pacific

SHIN-ICHI KAMIKURI[1], THEODORE C. MOORE[2], HIROKI MATSUI[3] AND HIROSHI NISHI[4]

[1]*Faculty of Education, Ibaraki University, 2-1-1 Bunkyo, Mito, Ibaraki 310-8512, Japan (e-mail: shin-ichi.kamikuri.millefeuille@vc.ibaraki.ac.jp)*
[2]*Department of Earth and Environmental Sciences, University of Michigan, 1100 North University, Ann Arbor, Michigan 48109-1005, USA*
[3]*Center for Advanced Marine Core Research, Kochi University, B200 Monobe, Nankoku, Kochi 783-8502, Japan*
[4]*The Center for Academic Resources and Archives, Tohoku University Museum, Tohoku University, 6-3 Aoba, Aramaki-aza, Aoba-ku, Sendai, Miyagi 980-8578, Japan*

Received March 14, 2018; Revised manuscript accepted November 29, 2018

Abstract. Sedimentary sequences obtained from drilling during Integrated Ocean Drilling Program (IODP) Expedition 320/321, "Pacific Equatorial Age Transect (PEAT)" at eight sites (Sites U1331–1338) in the equatorial Pacific offer an ideal record for reconstructing the evolution of the ocean/climate system throughout the Cenozoic. The sediments drilled at Site U1335 record short-term events of paleoceanographic significance, including the early Miocene climatic optimum (MCO) and the middle Miocene climatic transition (MMCT). Abundant well preserved radiolarians were recovered from the lower Miocene radiolarian Zone RN2 through middle Miocene Zone RN5 at IODP Site U1335. A total of 46 radiolarian datum levels consisting of 20 first occurrences (FOs), 25 last occurrences (LOs), and one evolutionary transition (ET) was recognized within the studied interval at Site U1335. Of these datum levels, 36 radiolarian datum levels were directly tied to the geomagnetic polarity time scale (GPTS) across the early/middle Miocene boundary. The general magnitude of evolutionary change was estimated based on the total turnover rate (the sum of FOs and LOs per 0.5 m.y.) of tropical radiolarians, and two minor faunal turnovers of radiolarian species were recognized between 16.5 and 14.7 Ma and between 13.9 and 13.4 Ma. These faunal turnovers were associated with regional environmental changes such as the increased biological productivity in the equatorial Pacific during the MCO and the MMCT.

Key words: biological productivity, early Miocene climatic optimum (MCO), geomagnetic polarity time scale (GPTS), middle Miocene climatic transition (MMCT), total turnover rate

Introduction

Abrupt climatic changes are associated with a pulse of evolutionary turnover in terrestrial and marine biota (Wolfe, 1985; Raup and Sepkoski, 1986; Crowley and North, 1988; Thomas, 2007). The middle Miocene from *ca*. 17 to 12 Ma is one of the most important intervals in global climatic/oceanographic changes of the Neogene. The Neogene climatic optimum near the early/middle Miocene boundary from *ca*. 17 to 15 Ma was closely followed by global cooling in the early middle Miocene at *ca*. 14 Ma (Flower and Kennett, 1995; Holbourn *et al*., 2014, 2015). Marine sedimentary records from this period are characterized by large positive excursions in benthic foraminiferal oxygen isotopes, which are inferred to reflect the combination of Antarctic ice sheet growth and deep-water cooling (Flower and Kennett, 1995; Billups and Schrag, 2002; Zachos *et al*., 2008). Magnesium/calcium data from planktonic foraminifera demonstrate that sea surface temperatures cooled 6 to 7°C during the earliest middle Miocene in the Southern Ocean (Shevenell *et al*., 2004). Planktonic foraminiferal oxygen isotopes from the equatorial Pacific also indicate major cooling of surface water during the earliest middle Miocene (e.g. Matsui *et al*., 2017). In addition, the thermocline depth of the equatorial Pacific shoaled across the early/middle Miocene boundary due to the strength of the equatorial upwelling (e.g. Kamikuri and Moore, 2017; Matsui *et al*., 2017). Among the main potential controlling factors of the middle Miocene climate change are volcanism, intensity of chemical weathering, organic carbon burial, and tectonism, as well as ocean circulation changes (Flower and Kennett, 1995; Kuhnt *et al*., 2004; Potter and Szatmari, 2009; Butzin *et al*., 2011; Montes *et al*., 2015; Tada *et al*., 2016; De Vleeschouwer *et al*., 2017; Betzler *et al*., 2018). Volcanism and tectonism are related to Earth's inner magmatic activity, while chemical weathering is mainly related to monsoon activity; organic burial results from both monsoon and biological activity.

Radiolarians are unicellular holoplanktonic protozoa that are widely distributed in the oceans (e.g. Suzuki and Not, 2015). The relationships between radiolarian faunal turnover and major climatic/oceanographic changes have been discussed by several researchers so far. Lazarus (2002) documented that major turnover events during the mid-Miocene and end-Miocene (*ca.* 15–13 Ma and 7–4 Ma, respectively) coincide in timing with periods of major rapid cooling at high latitudes. On the other hand, Johnson and Nigrini (1985) identified 50 tropical radiolarian datum levels since the middle Miocene and suggested that many radiolarians evolved first in the Indian Ocean and later migrated to the western and eastern Pacific Ocean. Kamikuri *et al.* (2009) showed that relatively rapid replacement of tropical radiolarian species occurred near the middle/late Miocene boundary (*ca.* 10 Ma) in the equatorial Pacific. The faunal turnover of tropical radiolarians was associated with formation of the modern-like equatorial circulation system near the middle/late Miocene boundary (Kamikuri *et al.*, 2009). However, compared to the late Neogene, the response of tropical radiolarian turnover to environmental changes from the early to middle Miocene is poorly understood. It is necessary to obtain information on the timing and number of origination and extinction bioevents in the equatorial Pacific based on biostratigraphic studies during times of major climatic stress across the early/middle Miocene boundary in order to estimate the general magnitude of evolutionary change and discuss the response of tropical radiolarian turnover to environmental changes.

The Neogene radiolarian biostratigraphy has been developed through biostratigraphic studies of numerous deep-sea sediments, as well as detailed taxonomic studies. The basic framework of the tropical radiolarian biostratigraphy during the Neogene was established in the works of Riedel and Sanfilippo (1970, 1978), Nigrini (1971), Caulet (1979), Johnson *et al*. (1989), and Moore (1995). In tropical regions, over 120 radiolarian datum levels since the late middle Miocene have been directly tied to the geomagnetic polarity time scale (GPTS) (Johnson *et al*., 1989; Moore, 1995; Nigrini *et al*., 2006; Kamikuri *et al*., 2009). As a result, the tropical radiolarian biostratigraphy since the latest middle Miocene has become a primary tool for dating and correlating deep-sea sediments (Sanfilippo and Nigrini, 1998). Despite these advances, most radiolarian datum levels from the early to middle Miocene in the tropical regions are not yet directly calibrated to the GPTS. Stratigraphically useful radiolarian datum levels have been proposed by some researchers, and these radiolarian datum levels for the early and middle Miocene have only been correlated indirectly to the GPTS by second-order methods such as extrapolations from sediment accumulation rate diagrams using calcareous microfossils including planktonic foraminifera and calcareous nannofossils (Moore, 1995; Nigrini *et al*., 2006; Kamikuri *et al*., 2009).

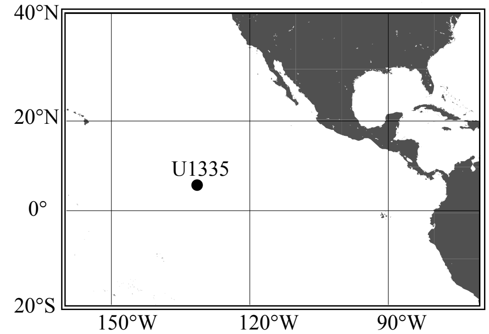

Figure 1. Location of Integrated Ocean Drilling Program (IODP) Expedition 320 Site U1335 in the tropical Pacific.

Recently, sedimentary sequences from the lower to middle Miocene with relatively high magnetic susceptibility were drilled at Site U1335 in the equatorial Pacific during IODP Expedition 320/321, "Pacific Equatorial Age Transect (PEAT)", and a paleomagnetic stratigraphy was established from the lower to middle Miocene in the obtained sequences (Pälike *et al*., 2010). Paleomagnetic stratigraphy provides an independent means of geochronology due to isochroneity of the Earth's magnetic reversal. The primary objective of this study is to directly correlate radiolarian datum levels with the GPTS for the early and middle Miocene time intervals at Site U1335 in the equatorial Pacific, after that to obtain information on the faunal turnover of tropical radiolarians in the equatorial Pacific based on the biostratigraphic studies during times of major climatic stress across the early/middle Miocene boundary.

Material and methods

During IODP Exp. 320/321, continuous sedimentary sequences were drilled at eight sites (Sites U1331 to U1338) in the low latitudes of the North Pacific (Pälike *et al.*, 2010). IODP Site U1335 (5°18.735′N, 126°17.002′W, water depth 4327.5 m; Figure 1) is located in the central area drilled during the PEAT and has ~420 m of sediments overlying the seafloor basalt. The position of Site U1335 was estimated to have ranged in latitude from about 0° to 2°N during the early and middle Miocene (Pälike *et al*., 2010). In this study, we use the CCSF-A (composite core depth below seafloor) spliced sediment depth scale (Pälike *et al*., 2010). The sedimentary sequence of the lower and middle Miocene is characterized by white to very pale brown and light greenish gray nannofossil

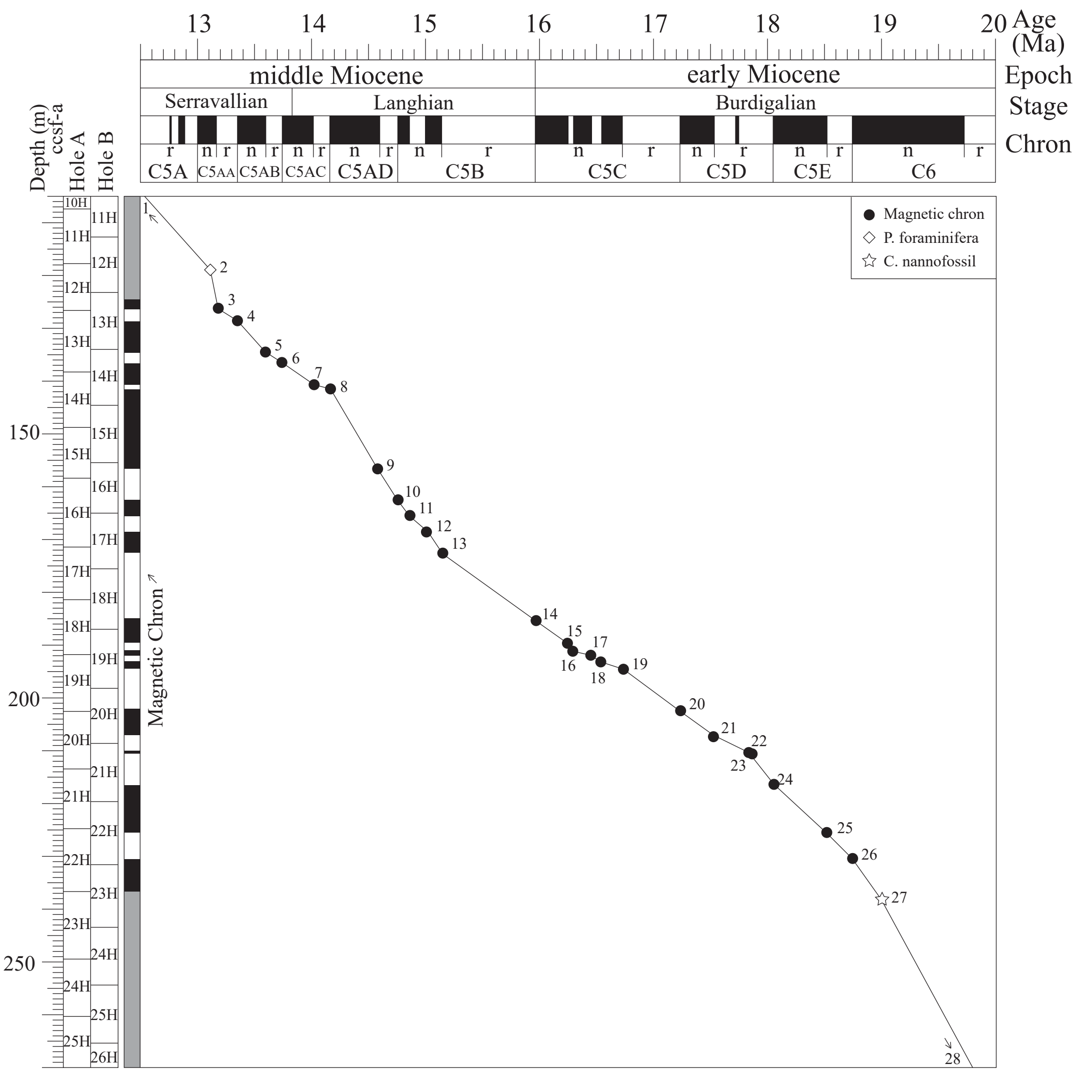

Figure 2. Age-depth plot for sedimentary sequences at Site U1335 based on paleomagnetic stratigraphy and nannofossil and planktonic foraminiferal biostratigraphy (Pälike *et al*., 2010). The time scale of Gradstein *et al*. (2012) is used in this study. Age control points are listed in Table 1.

ooze with well preserved siliceous microfossils including radiolarians and diatoms. Magnetic susceptibility is extremely low between 75 and 126 m CCSF-A and between 230 and 470 m CCSF-A (Pälike *et al*., 2010). These two intervals correspond to the light greenish gray nannofossil ooze.

High magnetic susceptibility is important for tie radiolarian datum levels to the paleomagnetic stratigraphy. We investigated the lower-middle Miocene sediments from 106.00 to 269.62 m CCSF-A at Site U1335 (Figure 2). Construction of the age-depth plot for the sedimentary sequences at Site U1335 was based on paleomagnetic stratigraphy and nannofossil and planktonic foraminiferal biostratigraphy (Pälike *et al.*, 2010) (Figure 2; Table 1). Paleomagnetic stratigraphy was established between 126 and 230 m CCSF-A across the lower/middle Miocene boundary at Site U1335 due to relatively high magnetic susceptibility. In the standard chronological scheme, the early/middle Miocene (Burdigalian/Langhian) boundary corresponds to the top of C5Cn.1n with an estimated age of 15.97 Ma (Gradstein *et al*., 2012). Hence, the early/middle Miocene boundary occurred at 184.045 m CCSF-A at Site U1335 (Figure 2; Pälike *et al.*, 2010). The time scale of Gradstein *et al*. (2012) was used in this study.

Investigations of radiolarian biostratigraphy were carried out at ~2.2 m intervals (spacing in time = ~0.1 m.y.) on a total of 74 sediment samples. Samples were sieved with 63 μm mesh and prepared following procedures

Table 1. Magnetic and biostratigraphic events used to construct the age-depth plot at Site U1335 (Pälike *et al*., 2010). Abbreviations: F, planktonic foraminifera; N, calcareous nannofossils; M, magnetic chrons; FO, first occurrence; LO, last occurrence.

Paleomagnetic/biostratigraphic events		Age (Ma)	Depth (m ccsf)		
			Hole 1335A	Hole 1335B	Midpoint
1. N	LO *Coronocyclus nitescens*	12.12	94.950		94.950
2. F	FO *Globorootalia fohsi robusta*	13.13	119.060		119.060
3. M	C5AAn-C5AAr	13.183		126.188	126.188
4. M	C5AAr-C5ABn	13.369		128.713	128.713
5. M	C5ABn-C5ABr	13.605		134.578	134.578
6. M	C5ABr-C5ACn	13.734		136.415	136.415
7. M	C5ACn-C5ACr	14.095		140.703	140.703
8. M	C5ACr-C5ADn	14.194		141.603	141.603
9. M	C5ADn-C5ADr	14.581		156.668	156.668
10. M	C5ADr-C5Bn.1n	14.784		162.380	162.380
11. M	C5Bn.1n-C5Bn.1r	14.877		165.530	165.530
12. M	C5Bn.1r-C5Bn.2n	15.032		168.555	168.555
13. M	C5Bn.2n-C5Br	15.16		172.468	172.468
14. M	C5Br-C5Cn.1n	15.974	184.045	186.248	185.147
15. M	C5Cn.1n-C5Cn.1r	16.268	189.595	189.673	189.634
16. M	C5Cn.1r-C5Cn.2n	16.303		191.023	191.023
17. M	C5Cn.2n-C5Cn.2r	16.472		192.010	192.010
18. M	C5Cn.2r-C5Cn.3n	16.543	193.060	193.248	193.154
19. M	C5Cn.3n-C5Cr	16.721	194.323	194.423	194.373
20. M	C5Cr-C5Dn	17.235	202.793	201.943	202.368
21. M	C5Dn-C5Dr	17.533	207.105	207.018	207.062
22. M	C5Dr-C5Dr-1	17.825	210.005	210.088	210.047
23. M	C5Dr-1-C5Dr	17.853	210.655	210.675	210.665
24. M	C5Dr-C5En	18.056	216.520	216.475	216.498
25. M	C5En-C5Er	18.524	225.230	225.795	225.513
26. M	C5Er-C6n	18.748	230.430		230.430
27. N	FO *Sphenolithus belemnos*	19.03	238.150		238.150
28. N	TC *Triquetrorhabdulus carinatus*	22.09	367.920		367.920

similar to those described by Sanfilippo *et al*. (1985). Briefly, sediment samples were treated with 15% H_2O_2 to remove organic material, treated with 15% HCl solution to remove the calcareous fraction, washed, and sieved with 63 μm mesh. Residues were randomly settled on a slide (Moore, 1973) and covered with a 24 × 40 mm cover glass with Norland Optical Adhesive #61 as the mounting medium. All radiolarian skeletons on the slides were observed under a light microscope at ×100 to ×250 magnification.

Preservation of radiolarian shells was classified as good (G), having only minor fragmentation; moderate (M), having obvious fragmentation, but without impairing identification of species; and poor (P), having considerable fragmentation in individual taxa with identification of some species not possible (Appendix). All specimens mounted on a slide were observed to confirm the occurrence of stratigraphic marker species. We counted stratigraphically useful taxa based on systematic examination of 500 radiolarians per sample (Appendix), and after that, observed all specimens on a slide to confirm the occurrence of stratigraphic marker species. Abbreviations were defined as follows: abundant (A), >10%; common (C), >5 to 10%; few (F), 1 to 5%; rare (R), <1%: present (*), present in a slide, but outside of area counted. We principally used the first and last occurrences of morphotypes and included evolutionary transitions between morphotypes within a lineage. The radiolarian species list with microphotographs is available in Kamikuri (2019).

Results

Radiolarian biostratigraphy across the early/middle Miocene boundary

A total of 46 radiolarian bioevents consisting of 20 first occurrences (FOs), 25 last occurrences (LOs), and one evolutionary transition (ET) were recognized in the studied interval at Site U1335 (Figure 3; Table 2). In this study, 36 radiolarian datum levels were directly tied to the GPTS across the early/middle Miocene boundary, but 10 radiolarian datum levels remain indirectly calibrated to the GPTS via calcareous microfossils because a paleomagnetic stratigraphy was not established in intervals other than 126 to 230 m CCSF-A at Site U1335 due to extremely low magnetic susceptibility (Figure 2; Table 1).

Sanfilippo and Nigrini (1998) standardized and introduced code numbers for the radiolarian zonation for the tropical Pacific, Indian and Atlantic oceans (RN1-RN17 for the Neogene) to facilitate communication between biostratigraphers and other geologists. In this study, the standard tropical zonation of Sanfilippo and Nigrini (1998) was applied based on the presence of well preserved tropical radiolarians in deep-sea sediments at Site U1335. As mentioned below, the target time interval at Site U1335 was divided into four radiolarian zones from RN2 to RN5 (19.8 to 12.6 Ma) (Figure 3).

Dorcadospyris alata Interval Zone (RN5)

Author.—Riedel and Sanfilippo (1970), modified by Riedel and Sanfilippo (1978).

Definition.—Interval from the FO of *Diartus petterssoni* (top) to the ET from *Dorcadospyris dentata* to *Dorcadospyris alata* (base).

Age.—11.9 Ma (Kamikuri *et al*., 2009) to 15.1 Ma (this study).

Chronology.—The top is at the lowermost part of C5r.3r (Kamikuri *et al*., 2009), the base is in C5Bn.2n (Figure 3).

Base interval.—U1335A-16H-CC through U1335A-17H-2, 105-107 cm (167.83 through 173.95 m CCSF-A).

Secondary biohorizons.—Three FOs (*Dictyophimus splendens*, *Lithopera neotera* and *Pterocanium* sp. A) and 13 LOs (*Calocycletta costata*, *Calocycletta robusta*, *Calocycletta virginis*, *Carpocanopsis bramlettei*, *Didymocyrtis bassanii*, *Didymocyrtis mammifera*, *Didymocyrtis tubaria*, *Dorcadospyris dentata*, *Eucoronis octopylus*, *Liriospyris parkerae*, *Liriospyris stauropora*, *Stichocorys armata*, and *Valkyria pukapuka*) (Figure 3; Table 2).

Remarks.—Eight LOs are located within magnetic chron C5ABn. The top of this zone is not recognized in this study due to being out of range of the studied samples.

Calocycletta (Calocyclissima) costata Interval Zone (RN4)

Author.—Riedel and Sanfilippo (1970), modified by Riedel and Sanfilippo (1978).

Definition.—Interval from the ET from *Dorcadospyris dentata* to *Dorcadospyris alata* (top) to the FO of *Calocycletta costata* (base).

Age.—15.1 to 17.1 Ma (Table 2).

Chronology.—The top is within C5B.2n, and the base is within the lower part of C5Cr (Figure 3).

Base interval.—U1335A-19H-4, 105-107 cm through 1335A-19H-CC (197.26 through 201.72 m CCSF-A).

Secondary biohorizons.—Nine FOs (*Calocycletta caepa*, *Carpocanopsis cristata*, *Didymocyrtis laticonus*, *Dorcadospyris alata*, *Eucoronis octopylus*, *Eucoronis perspicillum*, *Eucoronis toxarium*, *Liriospyris parkerae*, and *Lithopera renzae*) and eight LOs (*Carpocanopsis cingulata*, *Collosphaera glebulenta*, *Didymocyrtis prismatica*, *Didymocyrtis violina*, *Dorcadospyris forcipata*, *Lychnocanoma elongata*, *Lychnocanoma* sp. A, and *Stichocorys diaphanes*) (Figure 3; Table 2).

Remarks.—Five FOs are located within Chron C5Cn.2r, and seven LOs are within C5Br. The early/middle Miocene boundary (15.97 Ma) is approximately coincident with the LO of *Lychnocanoma* sp. A at Site U1335 (Figure 3; Table 2).

Stichocorys wolffii Interval Zone (RN3)

Author.—Riedel and Sanfilippo (1978).

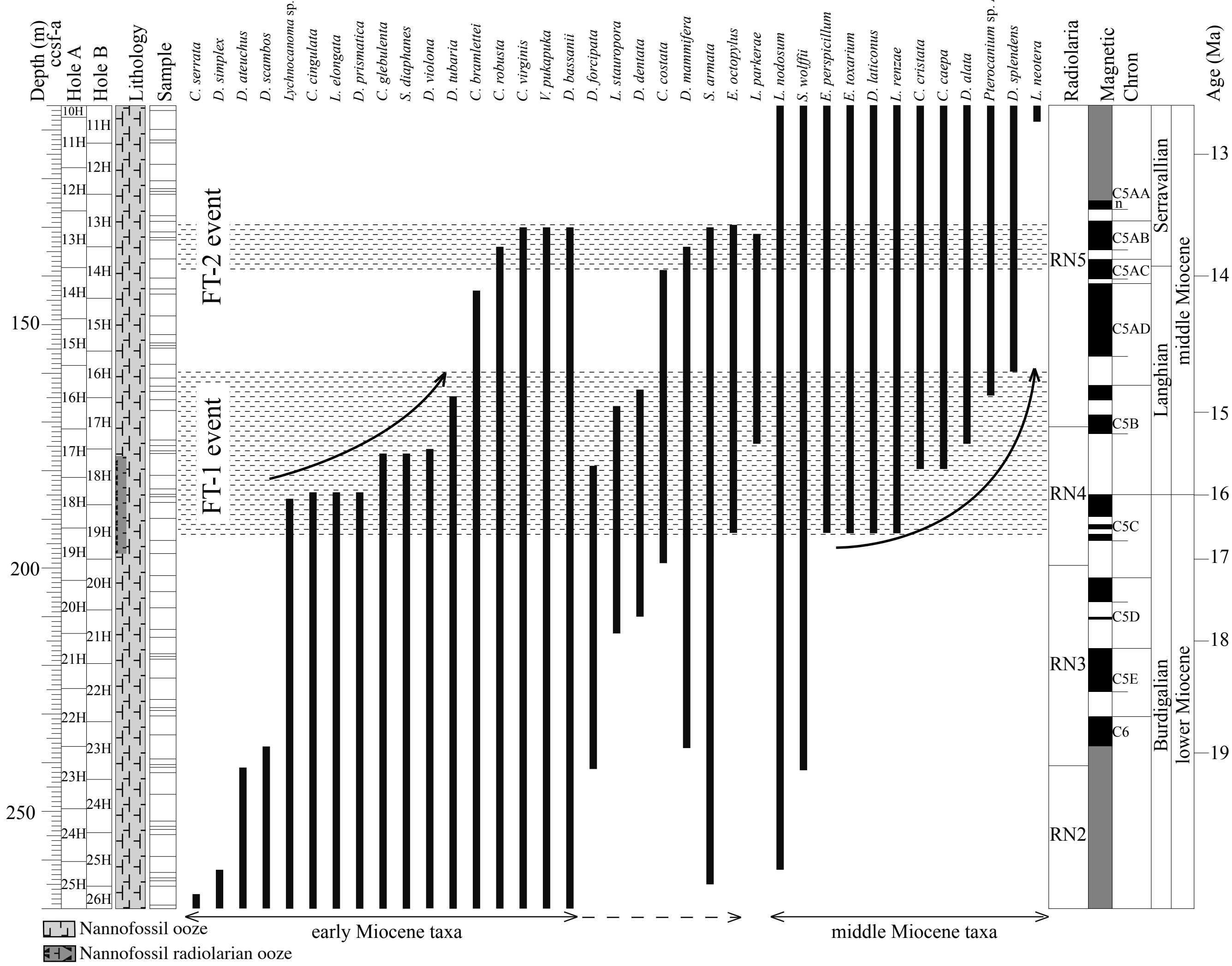

Figure 3. Stratigraphic distribution of selected radiolarian species across the early/middle Miocene boundary at Site U1335. Two minor faunal turnovers of radiolarian species occurred across the early/middle Miocene boundary and the earliest middle Miocene (between 16.5 and 14.7 Ma and between 13.9 and 13.4 Ma). Magnetostratigraphic results at this site are adapted from Pälike *et al*. (2010). Abbreviations: FT-1, faunal turnover-1; FT-2, faunal turnover-2.

Definition.—Interval from the FO of *Calocycletta costata* (top) to the FO of *Stichocorys wolffii* (base).

Age.—17.1 to 19.1 Ma (Table 2).

Chronology.—The top is within the lower part of C5Cr, and the base is within the upper part of the C6n (Figure 3).

Base interval.—U1335A-23H-3, 149-150 cm through U1335A-23H-4, 104-106 cm (241.31 through 242.36 m CCSF-A).

Secondary biohorizons.—Four FOs (*Dorcadospyris dentata*, *Dorcadospyris forcipata*, *Didymocyrtis mammifera*, and *Liriospyris stauropora*) and two LOs (*Dorcadospyris ateuchus* and *Dorcadospyris scambos*) (Figure 3; Table 2).

Remarks.—There are fewer radiolarian datum levels in RN3 than in RN4 at Site U1335 in the eastern equatorial Pacific (Figure 3).

Stichocorys delmontensis Interval Zone (RN2)

Author.—Riedel and Sanfilippo (1978).

Definition.—Interval from the FO of *Stichocorys wolffii* (top) to the LO of *Theocyrtis annosa* (base).

Age.—19.1 Ma (this study) to 21.7 Ma (Kamikuri *et al*., 2005).

Chronology.—The top is the upper part of the C6n

Table 2. Radiolarian biostratigraphic events across the early/middle Miocene boundary at Site U1335 in the equatorial Pacific. Abbreviations: FO, first occurrence; LO, last occurrence; ET, evolutionary transition.

			Core, Section, interval (cm)		Depth (m-ccsf)			Age (Ma)		
Zone		Radiolarian datum	Top	Bottom	Top	Bottom	Midpoint	Top	Bottom	Midpoint
RN5	FO	*Lithopera neotera*	A-10H-CC	A-11H-2, 104-106	106.00	109.82	107.91	12.58	12.74	12.66
	LO	*Valkyria pukapuka*	A-13H-2, 105-107	A-13H-3, 149-150	129.18	131.13	130.16	13.39	13.47	13.43
	LO	*Liriospyris parkerae*	A-13H-3, 149-151	A-13H-4, 104-106	131.13	132.18	131.66	13.47	13.51	13.49
	LO	*Calocycletta virginis*	A-13H-2, 105-107	A-13H-3, 149-150	129.18	131.13	130.16	13.39	13.47	13.43
	LO	*Eucoronis octopylus* (upper)	A-13H-2, 105-107	A-13H-3, 149-150	129.18	131.13	130.16	13.39	13.47	13.43
	LO	*Stichocorys armata*	A-13H-2, 105-107	A-13H-3, 149-150	129.18	131.13	130.16	13.39	13.47	13.43
	LO	*Didymocyrtis bassanii*	A-13H-2, 105-107	A-13H-3, 149-150	129.18	131.13	130.16	13.39	13.47	13.43
	LO	*Didymocyrtis mammifera*	B-13H-CC	A-13H-CC	133.05	136.63	134.84	13.54	13.75	13.65
	LO	*Calocycletta robusta*	B-13H-CC	A-13H-CC	133.05	136.63	134.84	13.54	13.75	13.65
	LO	*Calocycletta costata*	A-13H-CC	A-14H-2, 105-107	136.63	140.75	138.69	13.75	14.10	13.93
	LO	*Carpocanopsis bramlettei*	A-14H-4, 105-107	B-14H-CC	143.75	143.75	143.75	14.25	14.25	14.25
	FO	*Dictyophimus splendens*	A-15H-CC	A-16H-2, 115-117	158.43	160.90	159.66	14.64	14.73	14.69
	LO	*Dorcadospyris dentata*	A-16H-3, 149-150	A-16H-4, 115-117	162.74	163.90	163.32	14.79	14.83	14.81
	FO	*Pterocanium* sp. A	A-16H-4, 115-117	B-16H-CC	163.90	165.45	164.67	14.83	14.87	14.85
	LO	*Didymocyrtis tubaria*	A-16H-4, 115-117	B-16H-CC	163.90	165.45	164.67	14.83	14.87	14.85
	LO	*Liriospyris stauropora*	B-16H-CC	A-16H-CC	165.45	167.83	166.64	14.87	14.99	14.93
	ET	*D. dentata* > *D. alata*	A-16H-CC	A-17H-2, 105-107	167.83	173.95	170.89	14.99	15.25	15.12
RN4	FO	*Dorcadospyris alata*	A-17H-2, 105-107	B-17H-CC	173.95	174.92	174.43	15.25	15.32	15.29
	FO	*Liriospyris parkerae*	A-17H-2, 105-107	B-17H-CC	173.95	174.92	174.43	15.25	15.32	15.29
	LO	*Didymocyrtis violina*	A-17H-2, 105-107	B-17H-CC	173.95	174.92	174.43	15.25	15.32	15.29
	LO	*Stichocorys diaphanes*	A-17H-3, 149-150	A-17H-4, 105-107	175.89	176.95	176.42	15.38	15.45	15.41
	LO	*Collosphaera glebulenta*	A-17H-3, 149-150	A-17H-4, 105-107	175.89	176.95	176.42	15.38	15.45	15.41
	FO	*Carpocanopsis cristata*	A-17H-4, 105-107	A-17H-CC	176.95	181.19	179.07	15.45	15.72	15.58
	FO	*Calocycletta caepa*	A-17H-4, 105-107	A-17H-CC	176.95	181.19	179.07	15.45	15.72	15.58
	LO	*Dorcadospyris forcipata*	A-17H-4, 105-107	A-17H-CC	176.95	181.19	179.07	15.45	15.72	15.58
	LO	*Carpocanopsis cingulata*	A-18H-2, 105-107	B-18H-CC	183.92	185.08	184.50	15.90	15.97	15.93
	LO	*Lychnocanoma elongata*	A-18H-2, 105-107	B-18H-CC	183.92	185.08	184.50	15.90	15.97	15.93
	LO	*Didymocyrtis prismatica*	A-18H-2, 105-107	B-18H-CC	183.92	185.08	184.50	15.90	15.97	15.93
	LO	*Lychnocanoma* sp. A	B-18H-CC	A-18H-3, 149-150	185.08	185.86	185.47	15.97	16.02	16.00
	FO	*Eucoronis toxarium*	A-18H-CC	A-19H-2, 105-107	190.19	194.26	192.22	16.28	16.70	16.49
	FO	*Eucoronis octopylus* (upper)	A-18H-CC	A-19H-2, 105-107	190.19	194.26	192.22	16.28	16.70	16.49
	FO	*Didymocyrtis laticonus*	A-18H-CC	A-19H-2, 105-107	190.19	194.26	192.22	16.28	16.70	16.49
	FO	*Lithopera renzae*	A-18H-CC	A-19H-2, 105-107	190.19	194.26	192.22	16.28	16.70	16.49
	FO	*Eucoronis perspicillum*	A-18H-CC	A-19H-2, 105-107	190.19	194.26	192.22	16.28	16.70	16.49
	FO	*Calocycletta costata*	A-19H-4, 105-107	A-19H-CC	197.26	201.72	199.49	16.91	17.19	17.05
RN3	FO	*Dorcadospyris dentata*	B-20H-CC	A-20H-CC	208.38	212.60	210.49	17.66	17.92	17.79
	FO	*Liriospyris stauropora*	A-20H-CC	A-21H-1, 105-107	212.60	214.57	213.58	17.92	17.99	17.95
	FO	*Didymocyrtis mammifera*	A-22H-CC	A-23H-2, 104-106	234.63	239.36	236.99	18.90	19.06	18.98
	LO	*Dorcadospyris scambos*	A-22H-CC	A-23H-2, 104-106	234.63	239.36	236.99	18.90	19.06	18.98
	LO	*Dorcadospyris ateuchus*	B-23H-CC	A-23H-3, 149-150	240.70	241.31	241.00	19.09	19.10	19.10
	FO	*Dorcadospyris forcipata*	A-23H-3, 149-150	A-23H-4, 104-106	241.31	242.36	241.83	19.10	19.13	19.12
	FO	*Stichocorys wolffii*	A-23H-3, 149-150	A-23H-4, 104-106	241.31	242.36	241.83	19.10	19.13	19.12
RN2	FO	*Lychnocanoma nodosum*	A-24H-CC	A-25H-2, 104-106	259.47	262.71	261.09	19.53	19.61	19.57
	LO	*Dorcadospyris simplex*	A-24H-CC	A-25H-2, 104-106	259.47	262.71	261.09	19.53	19.61	19.57
	FO	*Stichocorys armata*	A-25H-2, 104-106	B-25H-CC	262.71	263.96	263.34	19.61	19.64	19.62
	LO	*Calocycletta serrata*	A-25H-4, 104-106	A-25H-CC	265.71	269.62	267.67	19.68	19.77	19.73

(Figure 3), and the base is within C6AAr.2r (Kamikuri *et al*., 2005).

Secondary biohorizons.—Two FOs (*Lychnocanoma nodosum* and *Stichocorys armata*) and two LOs (*Calocycletta serrata* and *Dorcadospyris simplex*) (Figure 3; Table 2).

Remarks.—The base of this zone is not recognized in this study due to being out of range of the studied samples.

Radiolarian faunal turnover across the early/middle Miocene boundary

A total of 46 radiolarian bioevents consisting of 20 FOs, 25 LOs, and one ET were recognized within the studied interval at Site U1335 (Figure 3; Table 2). Of these, 11 FOs and 11 LOs placed between C5Cn.3n and C5ADr (between 16.5 and 14.7 Ma) across the early/middle Miocene boundary in the equatorial Pacific. On the other hand, nine LOs were focused between C5ACn and C5AB (between 13.9 and 13.4 Ma). Within this interval, the FO of radiolarian species was not observed in this study. Taken together, two faunal turnovers of radiolarian species occurred across the early/middle Miocene boundary (from 16.5 to 14.7 Ma) and the late middle Miocene (from 13.9 to 13.4 Ma) (Figure 3). In this study, the former is called the faunal turnover-1 (FT-1) event and the latter is called the faunal turnover-2 (FT-2) event. The FT-1 event is mainly characterized by the extinction of early Miocene taxa and origination of middle Miocene taxa, and the FT-2 event is marked only by extinction events of early Miocene and transition taxa (Figure 3). Although a faunal turnover is at least a partial replacement of the existing fauna, the term is also used for a minor extinction event just like the FT-2 event in this study.

Discussion

Faunal/floral turnover across the early/middle Miocene boundary (FO, LO, and total turnover rate) in the equatorial Pacific

Lazarus (2002) discussed radiolarian faunal turnover in terms of a total turnover rate (TTR; the sum of FOs and LOs per 0.5 m.y.). In this study, we applied this concept and calibrated the TTR of radiolaria, diatoms, planktonic foraminifera, and calcareous nannofossils for data of this study and previous studies. We assume a TTR lower than 2 events as low and a TTR higher than 5 events as high.

Radiolaria.—A total of 46 radiolarian bioevents consisting of 20 FOs, 25 LOs, and one ET was recognized within the studied interval at Site U1335 (Figure 3; Table 2). A plot of the number of FOs and LOs of radiolarian taxa in 0.5 m.y. increments in the equatorial Pacific from 20.0 to 12.5 Ma (Figure 4) shows that prior to 16.0 Ma, the number of LOs of radiolarians was generally low (<2 events per 0.5 m.y.), followed by two peaks in LO of radiolarians (5 to 6 events per 0.5 m.y.) between 16.0 and 15.5 Ma and between 13.5 and 13.0 Ma. In addition, three LOs per 0.5 m.y. also occurred in three intervals from 16.0 to 12.5 Ma. On the other hand, the number of FOs of radiolarians in the equatorial Pacific was generally low (<2 events per 0.5 m.y.) with an exception being the FOs of five radiolarian taxa between 16.5 and 16.0 Ma (Figure 4).

The TTR of radiolarians in the equatorial Pacific is shown in Figure 5. During the early to middle Miocene, relatively high TTR (5 to 7 per 0.5 m.y.) of radiolarians in the equatorial Pacific was recognized in two intervals between 16.5 and 14.5 Ma and between 13.5 and 13.0 Ma, and relatively low TTR (0 to 2 per 0.5 m.y.) occurred between 18.5 and 16.5 Ma and between 14.5 and 14.0 Ma. As mentioned above, two high TTR (faunal turnovers) of radiolarian species occurred across the early/middle Miocene boundary and the late middle Miocene. The former corresponds to the FT-1 event (from 16.5 to 14.7 Ma) and the latter corresponds to the FT-2 event (from 13.9 to 13.4 Ma) (Figures 3, 5).

Diatoms.—Barron (2003) reported the timing and number of FOs and LOs of planktonic diatoms from 18.5 Ma to the present in the equatorial Pacific. Prior to 14.0 Ma, the number of FOs of diatoms did not exceed two events per 0.5 m.y., an exception being the FO of five diatom taxa between 17.0 and 16.5 Ma (Figure 4). During the middle Miocene, between 14.0 and 12.5 Ma, the number of FOs of diatoms indicated three to six events per 0.5 m.y. in the equatorial Pacific. Throughout this studied interval, the number of LOs of diatoms was generally low (<2 events per 0.5 m.y.), except for an interval between 16.5 and 16.0 Ma (3 events per 0.5 m.y.) (Figure 4).

The TTR of diatoms in the equatorial Pacific from 20.0 to 12.5 Ma is plotted in Figure 5 using the data from Barron (2003). Relatively high TTR (5 to 7 per 0.5 m.y.) of diatoms occurred during two intervals, between 17.0 and 16.5 Ma and between 14.0 and 13.5 Ma in the equatorial Pacific.

Planktonic foraminifera and calcareous nannofossils.—The number of FOs and LOs of planktonic foraminifers and calcareous nannofossils in the equatorial Pacific is plotted in Figure 4 using data from the biochronologic studies of Pälike *et al*. (2010). The number of FOs and LOs of planktonic foraminifers and calcareous nannofossils was generally low (<2 events per 0.5 m.y.), except for during an interval between 14.0 and 13.0 Ma (3 to 4 LOs per 0.5 m.y.).

The TTR of planktonic foraminifera in the equatorial regions was generally low, but two small peaks (3 to 4 per 0.5 m.y.) were recognized between 15.0 and 14.5 Ma and between 13.5 and 13.0 Ma (Figure 5). For calcareous

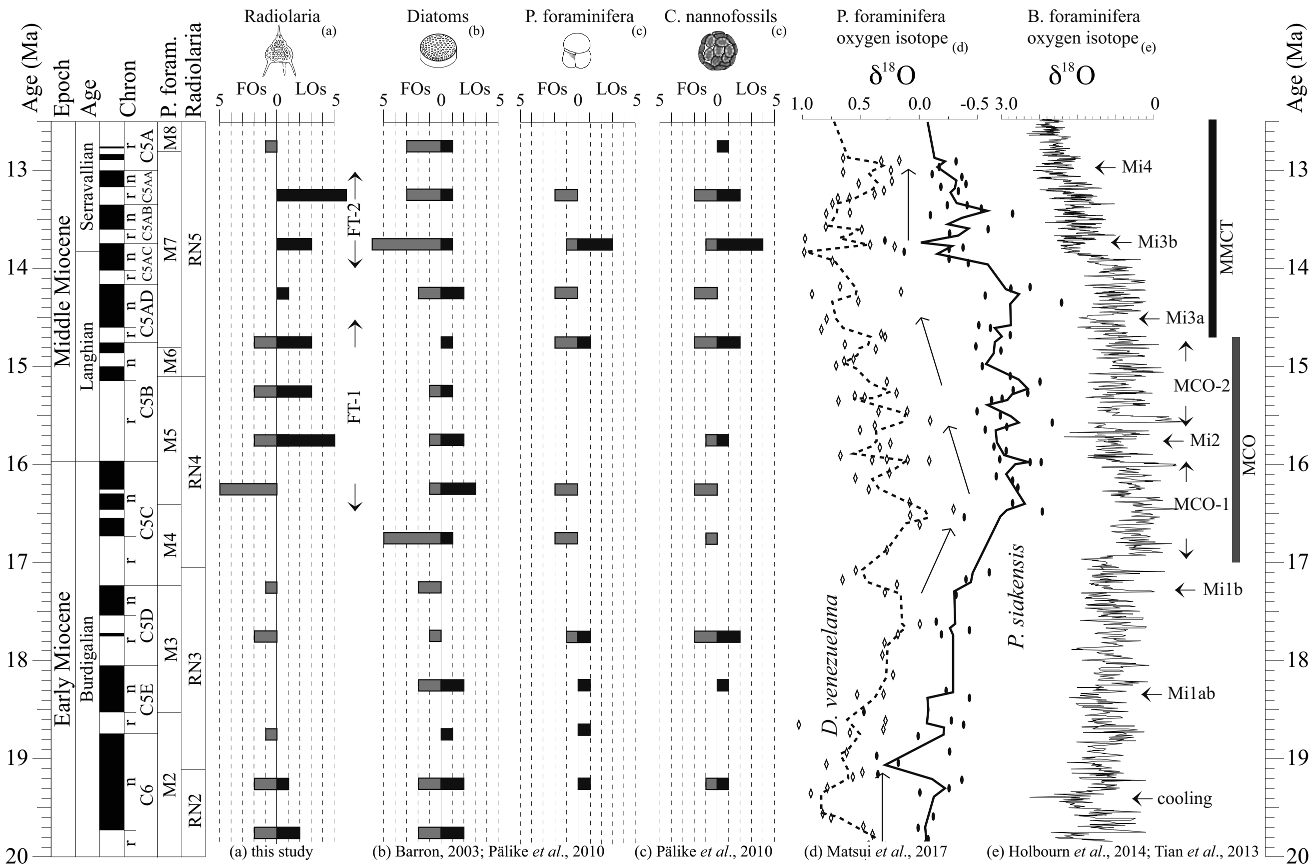

Figure 4. Number of first occurrences (FOs) and last occurrences (LOs) per 0.5 m.y. for radiolaria, diatoms, planktonic foraminifera, and calcareous nannofossils compared to published planktonic and benthic foraminiferal $\delta^{18}O$ values in the equatorial Pacific. The isotope events are from Miller *et al*. (1991), Billups and Schrag (2002), and Pekar and DeConto (2006). The so-called early Miocene climatic optimum (MCO) is divided into two intervals (MCO-1 and MCO-2) by the Mi2 event (Kamikuri and Moore, 2017). Abbreviations: MCO, early Miocene climatic optimum; MMCT, middle Miocene climatic transition. (a) this study; (b) Barron (2003) and Pälike *et al.* (2010); (c) Pälike *et al.* (2010); (d) Matsui *et al.*, 2017; (e) Holbourn *et al.*, 2014.

nannofossils, a relatively high TTR (4 to 5 per 0.5 m.y.) occurred between 14.0 and 13.0 Ma, and a small peak (4 per 0.5 m.y.) was found between 15.0 and 14.5 Ma. The patterns of TTR of calcareous nannofossils appear to be relatively similar to those of planktonic foraminifers (Figure 5).

Causes of faunal/floral turnover from the early to middle Miocene

Relatively high TTR peaks were identified in radiolaria and diatoms during the early Miocene climatic optimum (MCO) and the middle Miocene climatic transition (MMCT). On the other hand, the TTR of planktonic foraminifera and calcareous nannofossils showed two peaks during the MMCT. In this section, we discuss the plausible relation between faunal/floral turnover and environmental changes from the early to middle Miocene in the equatorial regions by comparing the TTR to environmental changes.

Faunal/floral turnover (16.5–14.7 Ma).—Radiolarians and diatoms, which are siliceous microfossils, had relatively high TTR in the equatorial Pacific from 16.5 to 14.7 Ma (Figures 3–5). The interval between *ca*. 17.0 and 14.7 Ma across the early/middle Miocene boundary was the warmest period in the Neogene and was identified as the MCO (Flower and Kennett, 1995; Billups and Schrag, 2002; Ogasawara *et al*., 2008; Oleinik *et al*., 2008; Zachos *et al*., 2008; Holbourn *et al*., 2015; Betzler *et al*., 2018). In the equatorial Pacific, the biological productivity increased with sea surface water warming during the MCO (Keller and Barron, 1983; Barron and Baldauf, 1990; Cortese *et al*., 2004; Shackford *et al*., 2012; Kamikuri and Moore, 2017; Matsui *et al*., 2017) (Figure 5).

It is difficult to interpret which environmental changes (global warming or increased biological productivity)

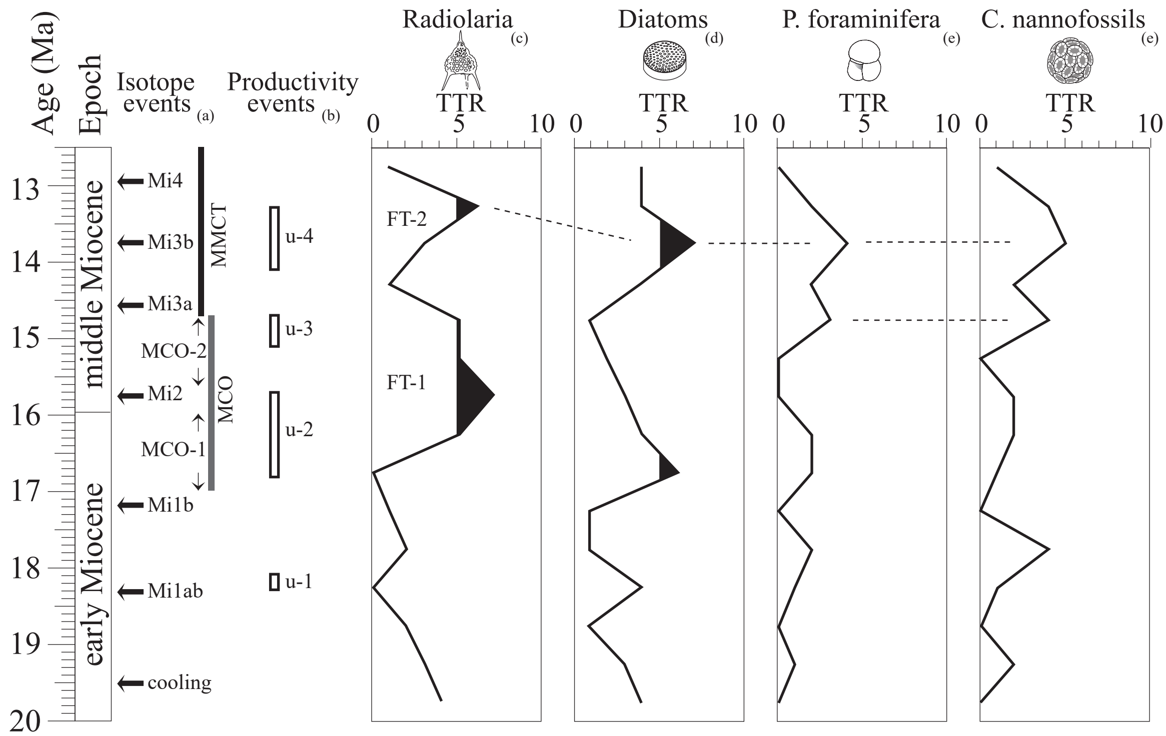

Figure 5. Total turnover rate (TTR; the sum of FOs and LOs per 0.5 m.y.) of radiolaria, diatoms, planktonic foraminifera, and calcareous nannofossils in the equatorial Pacific. The two relatively high TTR of radiolaria and diatoms were recognized in the MCO and MMCT, respectively. The two TTR peaks of planktonic foraminifera and calcareous nannofossils occurred during the MMCT. (a) Miller *et al.* (1991), Billups and Schrag (2002), Pekar and DeConto (2006), and Kamikuri and Moore (2017); (b) Kamikuri and Moore (2017); (c) this study; (d) Barron (2003); (e) Pälike *et al.* (2010).

were the major controlling factors of faunal/floral turnover in the equatorial Pacific. In the subarctic North Pacific and the Southern Ocean, faunal/floral turnovers (high TTR) in radiolarians and diatoms were not recognized during the MCO (Lazarus, 2002; Barron, 2003; Kamikuri *et al*., 2004, 2009). This may be also related to the fact that the accumulation pool of biogenic silica was the North Pacific Ocean at that time (e.g. Cortese *et al.*, 2004). Hence, regional environmental changes such as increased biological productivity might have affected the faunal/floral turnover of siliceous microfossils such as radiolarians and diatoms in the equatorial Pacific during the MCO (Figure 5). On the other hand, faunal/floral turnover of calcareous microfossils such as planktonic foraminifers and calcareous nannofossils was not found to have occurred in the equatorial Pacific during the MCO (Figure 5). Thus, the influence of environmental changes on calcareous microfossils and siliceous microfossils appears to have been different during the MCO in the equatorial Pacific.

Faunal/floral turnover (13.9–13.4 Ma).—A faunal/floral turnover among siliceous microfossils such as radiolaria and diatoms was recognized in the equatorial Pacific during the MMCT (Figure 5). The middle Miocene following the MCO represents a major change in Neogene climatic evolution and is designated the MMCT (Miller *et al*., 1991; Flower and Kennett, 1995; Billups and Schrag, 2002; Holbourn *et al*., 2014; Tada *et al.*, 2016; De Vleeschouwer *et al*., 2017). A large increase in benthic foraminiferal $\delta^{18}O$ during the MMCT from 14.7 to 12.9 Ma was interpreted as reflecting the major Antarctic Ice Sheet growth and a deep-water cooling (e.g. Woodruff and Savin, 1991; Billups and Schrag, 2002). The MMCT is characterized by three cooling steps at 14.7 Ma, 13.8 Ma, and 12.9 Ma, identified as Mi3a, Mi3b, and Mi4 events, respectively (Figure 4 in this study; Millet *et al*., 1991; Billups and Schrag, 2002). In the eastern equatorial Pacific, two massive increases in opal accumulation at *ca*. 14.0 Ma and *ca*. 13.8 Ma occurred just before and during the prominent cooling event (Mi3b) (Holbourn *et al*., 2014).

The faunal/floral turnover among siliceous microfossils was not recognized during the first step (Mi3a) in the equatorial Pacific, but one TTR peak was identified during the second cooling step (Mi3b) with high biological productivity (Figures 3 and 5). Hence, the high productivity with surface water cooling during Mi3b might be associated with the faunal/floral turnover in siliceous microfossils. On the other hand, calcareous microfossils such as planktonic foraminifera and calcareous nannofossils had experienced two minor faunal/floral turnover events in the equatorial Pacific during the first and second global cooling steps (Mi3a and Mi3b) of the MMCT (Figure 5). Hence, it is likely that global cooling events were associated with the two faunal/floral turnovers.

The number of extinction events in radiolarians and calcareous microfossils was relatively higher than that of origination events during the MMCT (Figure 5). During this interval, a decreased vertical thermal gradient in the equatorial Pacific (Matsui *et al*., 2017) might not have been conducive to species evolution (Figure 4). Unlike faunal/floral turnover for those two groups, however, diatom floral turnover in that interval was significantly marked by nine origination events in the equatorial Pacific (Figure 5). Low-latitude diatoms might have been able to adapt to global cooling relatively more quickly than other sorts of microplankton.

Conclusions

During IODP Expedition 320/321, continuous sedimentary sequences were drilled at eight sites (Sites U1331 to U1338) in the low latitudes of the North Pacific in order to reconstruct changes in the state, nature and variability of the Cenozoic oceanographic/climatic system in the equatorial Pacific. IODP Site U1335 is located in the central area drilled during the PEAT program and was selected in order to focus on the paleoceanographic changes from the late Oligocene to middle Miocene in the equatorial Pacific. The objective of this study was to directly correlate radiolarian datum levels with the GPTS for the early and middle Miocene time intervals at Site U1335 and to provide information on the faunal turnover of tropical radiolarians during times of major climatic stress across the early/middle Miocene boundary. The results are summarized below.

(1) The sedimentary sequence at Site 1335 was divided into four radiolarian zones from RN2 to RN5. A total of 46 radiolarian bioevents consisting of 20 FOs, 25 LOs, and one ET were recognized within the studied interval at Site U1335. In this study, 36 radiolarian datum levels were directly tied to the GPTS across the early/middle Miocene boundary.

(2) Two minor faunal turnovers of radiolarian species occurred across the early/middle Miocene boundary (16.5 to 14.7 Ma) and the late middle Miocene (13.9 to 13.4 Ma). In this study, the former is called the faunal turnover-1 (FT-1) event and the latter is called the faunal turnover-2 (FT-2) event. The FT-1 was characterized by 11 FOs and 11 LOs, and the FT-2 event was marked by nine LOs.

(3) The relatively high TTR of diatoms occurred in the equatorial Pacific during two intervals, between 17.0 and 16.5 Ma and between 14.0 and 13.5 Ma. The TTR of planktonic foraminifera in the equatorial regions was generally low, but two small peaks were recognized between 15.0 and 14.5 Ma and between 13.5 and 13.0 Ma. A relatively high TTR of calcareous nannofossils occurred between 14.0 and 13.0 Ma and a small peak was found between 15.0 and 14.5 Ma.

(4) Radiolarians and diatoms had relatively high TTR in the equatorial Pacific during the early MCO. Regional environmental changes such as increased biological productivity might have affected the faunal/floral turnover of siliceous microfossils in the equatorial Pacific. On the other hand, faunal/floral turnover in calcareous microfossils did not occur in the equatorial Pacific during the MCO. The influence of environmental changes on calcareous microfossils and siliceous microfossils appears to have been different during the MCO in the equatorial Pacific.

(5) Calcareous microfossils such as planktonic foraminifera and calcareous nannofossils experienced two minor faunal/floral turnovers in the equatorial Pacific during the first and second global cooling steps (Mi3a and Mi3b) of the MMCT. Global cooling events might be associated with the two faunal/floral turnovers in calcareous microfossils. On the other hand, faunal/floral turnover among siliceous microfossils such as radiolaria and diatoms was recognized as being related to a high productivity event during the second cooling step (Mi3b) in the equatorial Pacific. High productivity with surface water cooling during Mi3b might have been associated with faunal/floral turnover in siliceous microfossils.

(6) Unlike faunal/floral turnover in radiolarians, planktonic foraminifera, and calcareous nannofossils, diatom floral turnover was mainly marked by nine origination events in the equatorial Pacific. Low-latitude diatoms might have been able to adapt relatively more quickly than other sorts of microplankton to global cooling.

Acknowledgments

We are grateful to Heiko Pälike and the other scientists and crew members of Leg 320 of JOIDES Resolution for their support and prompt attention to our requests. Samples were provided by the Integrated Ocean Drilling Program (IODP). This work was also supported in part by the Japan Society for the Promotion of Science (JSPS) KAKENHI Grant Number 15K17780 (S. Kamikuri). We also wish to thank Isao Motoyama (Yamagata University) and Kenji M. Matsuzaki (University of Tokyo) for their reviews and valuable comments on the manuscript.

References

Barron, J. A., 2003: Planktonic marine diatom record of the past 18 m.y.: appearances and extinctions in the Pacific and southern oceans. *Diatom Research*, vol. 18, p. 203–224.

Barron, J. A. and Baldauf, J. G., 1990: Development of biosiliceous sedimentation in the North Pacific during the Miocene and early Pliocene. *In*, Tsuchi, R. *ed*., *Pacific Neogene Events: Their Timing, Nature and Interrelationship*, p. 43–63. University of Tokyo Press, Tokyo.

Betzler, C., Eberli, G. P., Lüdmann, T., Reolid, J., Kroon, D., Reijmer, J. J. G., Swart, P. K., Wright, J., Young, J. R., Alvarez-Zarikian, C., Alonso-Garcia, M., Bialik, O. M., Blättler, C. L., Guo, J. A., Haffen, S., Horozal, S., Inoue, M., Jovane, L., Lanci, L., Laya, J. C., Hui Mee, A. L., Nakakuni, M., Nath, B. N., Niino, K., Petruny, L. M., Pratiwi, S. D., Slagle, A. L., Sloss, C. R., Su, X. and Yao, Z., 2018: Refinement of Miocene sea level and monsoon events from the sedimentary archive of the Maldives (Indian Ocean). *Progress in Earth and Planetary Science*, vol. 5, p. 1–18.

Billups, K. and Schrag, D. P., 2002: Paleotemperatures and ice volume of the past 27 Myr revisited with paired Mg/Ca and ^{18}O/^{16}O measurements on benthic foraminifera. *Paleoceanography*, vol. 17. doi: 10.1029/2000PA000567.

Butzin, M., Lohmann, G. and Bickert, T., 2011: Miocene ocean circulation inferred from marine carbon cycle modeling combined with benthic isotope records. *Paleoceanography*, doi:10.1029/2009PA001901.

Caulet, J. P., 1979: Les dépôts à radiolaires d'age Pliocène supérieur à Pleistocène dans l'océan Indien central: nouvelle zonation biostratigraphique. *Mémoires du Muséum National d'Histoire Naturelle*, *série C43*, p. 119–141.

Cortese, G., Gersonde, R., Hillenbrand, C.-D. and Kuhn, G., 2004: Opal sedimentation shifts in the World Ocean over the last 15 Myr. *Earth and Planetary Science Letters*, vol. 224, p. 509–527.

Crowley, T. J. and North, G. R., 1988: Abrupt climate change and extinction events in earth history. *Science*, vol. 240, p. 996–1002.

De Vleeschouwer, D., Vahlenkamp, M., Crucifix, M. and Pälike, H., 2017: Alternating Southern and Northern Hemisphere climate response to astronomical forcing during the past 35 m.y. *Geology*, vol. 45, p. 375–378.

Flower, B. P. and Kennett, J. P., 1995: Middle Miocene deepwater paleoceanography in the southwest Pacific: Relations with East Antarctic Ice Sheet development. *Paleoceanography*, vol. 10, p. 1095–1112.

Gradstein, F. M., Ogg, J. G., Schmitz, M. D. and Ogg, G. M., 2012: *The Geologic Time Scale 2012*, 1144 p. Elsevier, Boston.

Holbourn, A., Kuhnt, W., Kochhann, K. G. D., Andersen, N. and Sebastian Meier, K. J., 2015: Global perturbation of the carbon cycle at the onset of the Miocene Climatic Optimum. *Geology*, vol. 43, p. 123–126.

Holbourn, A., Kuhnt, W., Lyle, M., Schneider, L., Romero, O. and Anderson, N., 2014: Middle Miocene climate cooling linked to intensification of eastern equatorial Pacific upwelling. *Geology*, vol. 42, p. 19–22.

Johnson, D. A. and Nigrini, C. A., 1985: Time-transgressive Late Cenozoic radiolarian events of the equatorial Indo-Pacific. *Science*, vol. 230, p. 538–540.

Johnson, D. A., Schneider, D. A., Nigrini, C. A., Caulet, J.-P. and Kent, D. V., 1989: Pliocene–Pleistocene radiolarian events and magnetostratigraphic calibrations for the tropical Indian Ocean. *Marine Micropaleontology*, vol. 14, p. 33–66.

Kamikuri, S., 2019: Radiolarian assemblages from the lower to middle Miocene at IODP Site U1335 in the eastern equatorial Pacific. *Bulletin of the Geological Survey of Japan*, vol. 70, p. 137–161.

Kamikuri, S. and Moore, T. C., 2017: Reconstruction of oceanic circulation patterns in the tropical Pacific across the early/middle Miocene boundary as inferred from radiolarian assemblages. *Palaeogeography*, *Palaeoclimatology*, *Palaeoecology*, vol. 487, p. 136–148.

Kamikuri, S., Motoyama, I., Nishi, H. and Iwai, M., 2009: Neogene radiolarian biostratigraphy and faunal evolution rates in the eastern equatorial Pacific ODP Sites 845 and 1241. *Acta Palaeontologica Polonica*, vol. 54, p. 713–742.

Kamikuri, S., Nishi, H., Moore, T. C. Jr., Nigrini, C. and Motoyama, I., 2005: Radiolarian faunal turnover across the Oligocene/Miocene boundary in the central eastern Pacific. *Marine Micropaleontology*, vol. 57, p. 74–96.

Kamikuri, S., Nishi, H., Motoyama, I. and Saito, S., 2004: Middle Miocene to Pleistocene radiolarian biostratigraphy in the Northwest Pacific, Ocean Drilling Program Leg 186. *Island Arc*, vol. 13, p. 191–226.

Keller, G. and Barron, J. A., 1983: Paleoceanographic implications of Miocene deep-sea hiatuses. *Geological Society of America*, *Bulletin*, vol. 94, p. 590–613.

Kuhnt, W., Holbourn, A., Hall, R., Zuvela, M. and Käse, R., 2004: Neogene history of the Indonesian throughflow. *In*, Clift, P. D., Kuhnt, W., Wang, P. and Hayes, E. *eds*., *Continent-Ocean Interactions within East Asian Marginal Seas*, p. 299–320. American Geophysical Union, Geophysical Monograph, vol. 149, Monograph American Geophysical Union, Washington.

Lazarus, D. B., 2002: Environmental control of diversity, evolutionary rates and taxa longevities in Antarctic Neogene Radiolaria. *Palaeontologia Electronica*, vol. 32, p. 1–32.

Matsui, H., Nishi, H., Kuroyanagi, A., Hayashi, H., Ikehara, M. and Takashima, R., 2017: Vertical thermal gradient history in the eastern equatorial Pacific during the early to middle Miocene: implications for the equatorial thermocline development. *Paleoceanography*, doi:10.1002/2016A003058.

Miller, K. G., Wright, J. D. and Fairbanks, R. G., 1991: Unlocking the ice house: Oligocene–Miocene oxygen isotopes, eustasy and margin erosion. *Journal of Geophysical Research*, vol. 96, p. 6829–6848.

Montes, C., Cardona, A., Jaramillo, C., Silva, J. C., Valencia, V., Pérez-Ayala, C., Angel, L. C., Rodriguez-Parra, L. A. and Niño, H., 2015: Middle Miocene closure of the Central American Seaway. *Science*, vol. 348, p. 226–228.

Moore, T. C. Jr., 1973: Method of randomly distributing grains for microscopic examination. *Journal of Sedimentary Petrology*, vol. 43, p. 904–906.

Moore, T. C. Jr., 1995: Radiolarian stratigraphy, Leg 138. *In*, Pisias, N. G. *et al*., *Proceedings of the Ocean Drilling Program*, *Scientific Results*, vol. 138, p. 191–232. Ocean Drilling Program, College Station.

Nigrini, C., 1971: Radiolarian zones in the Quaternary of the equatorial Pacific Ocean. *In*, Funnell, B. M. and Riedel, W. R. *eds*., *The Micropalaeontology of Oceans*, p. 443–461. Cambridge University Press, Cambridge.

Nigrini, C., Sanfilippo, A. and Moore, T. C. Jr., 2006: Cenozoic radiolarian biostratigraphy: a magnetobiostratigraphic chronology of Cenozoic sequences from ODP Sites 1218, 1219, and 1220, equatorial Pacific. *In*, Wilson, P. A., Lyle, M. and Firth, J. V. *eds*., *Pro-*

ceedings of the Ocean Drilling Program, Scientific Results, vol. 199, p. 1–76. Ocean Drilling Program, College Station.

Ogasawara, K., Takano, M., Nagato, H. and Nakano, T., 2008: Cenozoic molluskan faunas and climatic changes in the northern Pacific related to Pacific gateways: review and perspective. *Bulletin of the Geological Survey of Japan*, vol. 59, p. 355–364.

Oleinik, A., Marincovich, L. Jr., Barinov, K. B. and Swart, P. K., 2008: Magnitude of Middle Miocene warming in North Pacific high latitudes: stable isotope evidence from *Kaneharaia* (Bivalvia, Dosiniinae). *Bulletin of the Geological Survey of Japan*, vol. 59, p. 339–353.

Pälike, H., Nishi, H., Lyle, M., Raffi, I., Gamage, K., Klaus, A. and the Expedition 320/321 Scientists, 2010: Expedition 320/321 summary. *In*, Pälike, H., Lyle, M., Nishi, H., Raffi, I., Gamage, K., Klaus, A. and the Expedition 320/321 Scientists, *Proceedings of the Integrated Ocean Drilling Program*, vol. 320/321, p. 1–141. Integrated Ocean Drilling Program Management International, Inc., Tokyo.

Pekar, S. F. and DeConto, R. M., 2006: High-resolution ice-volume estimates for the early Miocene: Evidence for a dynamic ice sheet in Antarctica. *Palaeogeography*, *Palaeoclimatology*, *Palaeoecology*, vol. 231, p. 101–109.

Potter, P. E. and Szatmari, P., 2009: Global Miocene tectonics and the modern world. *Earth-Science Reviews*, vol. 96, p. 279–295.

Raup, D. M. and Sepkoski, J. J. Jr., 1986: Periodic extinctions of families and genera. *Science*, vol. 231, p. 833–836.

Riedel, W. R. and Sanfilippo, A., 1970: Radiolaria, Leg 4, Deep Sea Drilling Project. *In*, Bader, R. G., Gerard, R. D. *et al.*, *Initial Reports of the Deep Sea Drilling Project*, vol. 4, p. 503–575. U.S. Government Printing Office, Washington.

Riedel, W. R. and Sanfilippo, A., 1978: Stratigraphy and evolution of tropical Cenozoic radiolarians. *Micropaleontology*, vol. 24, p. 61–96.

Sanfilippo, A. and Nigrini, C., 1998: Code numbers for Cenozoic low latitude radiolarian biostratigraphic zones and GPTS conversion tables. *Marine Micropaleontology*, vol. 33, p. 109–156.

Sanfilippo, A., Westberg-Smith, M. J. and Riedel, W. R., 1985: Cenozoic radiolaria. *In*, Bolli, H. M., Saunders, J. B. and Perch-Nielsen, K. *eds.*, *Plankton Stratigraphy*, p. 631–712. Cambridge University Press, Cambridge.

Shackford, J. K., Lyle, M., Wilkens, R. and Tian, J., 2012: Data report: raw and normalized elemental data along the Site U1335, U1336, and U1337 splices from X-ray fluorescence scanning. *In*, Pälike, H., Lyle, M., Nishi, H., Raffi, I., Gamage, K., Klaus, A. and the Expedition 320/321 Scientists, *Proceedings of the Integrated Ocean Drilling Program*, vol. 320/321. Integrated Ocean Drilling Program Management International, Inc., Tokyo.

Shevenell, A. E., Kennett, J. P. and Lea, D. W., 2004: Middle Miocene Southern Ocean cooling and Antarctic cryosphere expansion. *Science*, vol. 305, p. 1766–1770.

Suzuki, N. and Not, F., 2015: Biology and ecology of Radiolaria. *In*, Ohtsuka, S., Suzaki, T., Horiguchi, T., Suzuki, N. and Not, F. *eds.*, *Marine Protists*, p. 179–222. Springer, Japan.

Tada, R., Zheng, H. and Clift, P. D., 2016: Evolution and variability of the Asian monsoon and its potential linkage with uplift of the Himalaya and Tibetan Plateau. *Progress in Earth and Planetary Science*, vol. 3, p. 1–26.

Thomas, E., 2007: Cenozoic mass extinctions in the deep sea: What perturbs the largest habitat on Earth? *Geological Society of America*, *Special Paper*, vol. 424, p. 1–23.

Tian, J., Yang, M., Lyle, M. W., Wilkens, R. and Shackford, J. K., 2013: Obliquity and long eccentricity pacing of the Middle Miocene climatic transition. *Geochemistry*, *Geophysics*, *Geosystems*, vol. 14, p. 1740–1755.

Wolfe, J. A., 1985: Distribution of major vegetational types during the Tertiary. *In*, Sundquist, E. T. and Broecker, W. S. *eds*., *The Carbon Cycle and Atmospheric* CO_2*: Natural Variations Archean to Present*, p. 357–375. American Geophysical Union, Geophysical Monograph Series, vol. 32, Monograph American Geophysical Union, Washington.

Woodruff, F. and Savin, S. M., 1991: Mid-Miocene isotope stratigraphy in the deep sea: high-resolution correlations, paleoclimatic cycles and sediment preservation. *Paleoceanography*, vol. 6, p. 755–806.

Zachos, J. C., Dickens, G. R. and Zeebe, R. E., 2008: An early Cenozoic perspective on greenhouse warming and carbon-cycle dynamics. *Nature*, vol. 451, p. 279–283.

Author contributions

Shin-ichi Kamikuri, who is Exp.320 participant, studied radiolarian biostratigraphy. Ted Moore, who is Exp.320 participant, studied radiolarian biostratigraphy with first author and was primarily responsible for the half of all sample. Hiroki Matsui carried out the geochemical analysis and its interpretation with faunal/floral turnover. Hiroshi Nishi, who is Exp.320 participant, summarized biostratigraphy of calcareous microfossil and discussed its interpretation. All authors contributed to the writing of the paper.

Appendix. Stratigraphic distribution of selected radiolarian taxa at Site U1335.

Hole	section, interval	Deoth (m csf-a)	Depth (m ccsf-a)	Age (Ma)	Preservation	1 *Calocycletta caepa* Moore	2 *Calocycletta costata* (Riedel)	3 *Calocycletta robusta* Moore	4 *Calocycletta serrata* Moore	5 *Calocycletta virginis* (Haeckel)	6 *Carpocanium bramlettei* (Riedel and Sanfilippo)	7 *Carpocanium cingulatum* (Riedel and Sanfilippo)	8 *Carpocanopsis cristata* (Carnevale)	9 *Collosphaera glebulenta* Bjørkuland and Goll	10 *Dictyophimus splendens* (Campbell and Clark)	11 *Didymocyrtis bassanii* (Carnevale)	12 *Didymocyrtis laticonus* (Riedel)	13 *Didymocyrtis mammifera* (Haeckel)	14 *Didymocyrtis prismatica* (Haeckel)	15 *Didymocyrtis tubaria* (Haeckel)	16 *Didymocyrtis violina* (Haeckel)	17 *Dorcadospyris alata* (Riedel)	18 *Dorcadospyris ateuchus* (Ehrenberg)	19 *Dorcadospyris dentata* Haeckel	20 *Dorcadospyris forcipata* (Haeckel)	21 *Dorcadospyris scambos* Moore and Nigrini	22 *Dorcadospyris simplex* (Riedel)	23 *Eucoronis octopylus* (Haeckel)	24 *Eucoronis perspicillum* Haeckel	25 *Eucoronis toxarium* (Haeckel)	26 *Liriospyris parkerae* Riedel and Sanfilippo	27 *Liriospyris stauropora* (Haeckel)	28 *Lithopera neotera* Sanfilippo and Riedel	29 *Lithopera renzae* Sanfilippo and Riedel	30 *Lychnocanoma elongata* (Vinassa de Regny)	31 *Lychnocanoma nodosum* (Haeckel)	32 *Lychnocanoma* sp. A	33 *Pterocanium* sp. A	34 *Stichocorys armata* (Haeckel)	35 *Stichocorys diaphanes* (Sanfilippo and Riedel)	36 *Stichocorys wolffii* Haeckel	37 *Valkyria pukapuka* O'Connor
A	10HCC	94.95	106.00	12.58	G	F							*		*		C					*							*	*			*	R		R		R			*	
A	11H-2, 104-106	96.96	109.82	12.74	G	F							*		*		F					*							*					R		R		R			*	
A	11H-2, 149-150	97.39	110.25	12.76	G	F							*				C												*	*				F		R		R			*	
B	11HCC	98.97	112.08	12.84	G	F							*				C													*				F		R		R				
A	11H-4, 104-106	99.95	112.81	12.87	G	F											C					*							*	*				R		R					*	
A	11HCC	104.17	117.03	13.04	G	R							*		*		C												*					R		*		R			*	
A	12H-2, 104-106	106.45	120.54	13.14	G	F							*				F					*							*	*				R		R						
A	12H-3, 150-152	108.39	122.48	13.16	M	R							*				F					*							*					R		R		R			*	
B	12HCC	108.08	122.58	13.16	G	F							*		*		F					*								*				R		R		R			*	
A	12H-4, 104-106	109.45	123.54	13.16	G	R							*				F					*							R	*				R		R		R				
A	12HCC	113.85	127.94	13.31	G	R							*		R		F					*							*	*				*		R		R			*	
A	13H-2, 104-106	115.94	129.18	13.39	M	R									*		F					*							R	F				R		R						
A	13H-3, 149-150	117.89	131.13	13.47	G	*				F			*			R	F					*						R	*	R				R		R		R	R		F	R
A	13H-4, 104-106	118.94	132.18	13.51	M	*				C			*			*	F					*						*		R	R					*			R		R	R
B	13HCC	117.65	133.05	13.54	G	R				F						R	C					*						*		*	R			R		*			F		*	R
A	13HCC	123.39	136.63	13.75	G	R		*		F			*		*	*	C	R				*						R	*		*			R		*		R	F		*	*
A	14H-2, 105-107	125.45	140.75	14.10	M	*	*	*		C			*				F	F				*						R	R		R			R		*			R		R	R
A	14H-3, 149-150	127.39	142.69	14.22	G	R	R	*		C			*			*	F	F				*						R	R		F			R		R		*	R		R	*
A	14H-4, 105-107	128.45	143.75	14.25	G	*	F	*		C			*		*	R	R	F				*						R	*	*	F			*		R			R		R	*
B	14HCC	127.01	143.75	14.25	G	*	F	*		C	R				*	R	R	F				R						R	*	R	F			R		R			R		R	*
A	14HCC	132.99	148.29	14.37	G	R	F	R		F	R		*		*	R	*	F				R						F	*	R	F			R		R		*	R		R	R
A	15H-3, 105-107	135.95	152.30	14.47	M	R		*		F	R		*			R	*	F				R						R	R	R	F			R		R		R	R		*	*

Appendix. *Continued 1.*

					No.	1	2	3	4	5	6	7	8	9	10	11	12	13	14	15	16	17	18	19	20	21	22	23	24	25	26	27	28	29	30	31	32	33	34	35	36	37
B	15HCC	136.78	154.14	14.52	G	R	*	*		F	R				*	R	*	C				R						R	*	R	F			R		R		*	R		R	*
A	15H-3, 149-150	137.89	154.24	14.52	G	R	*	*		F	R				*	*	*	C				*						R		R	F			R		R					F	*
A	15H-5, 105-107	138.95	155.30	14.55	G	*	R	*		C	*		*			R	*	F				*						R	*	R	R			R		R			R		F	R
A	15HCC	142.08	158.43	14.64	G	R	F	R		C	R				*	R	F	R				*						R	*	*	R			R		R			R		R	R
A	16H-2, 115-117	144.55	160.90	14.73	G	*	F	*		C	R		*			R	R	R				R						R	R	R	F			F		*		*	R		R	R
A	16H-3, 149-150	146.39	162.74	14.79	G	*	F	*		C	R					*	R	R				R						F	*	F	F			F		R					F	
A	16H-4, 115-117	147.55	163.90	14.83	G	R	F	F		F	F		*			R	R	F				*		*				R	R	R	F			R		R		*	R		R	R
B	16HCC	146.17	165.45	14.87	G	R	F	F		F	R					R	F	F		R		*						F	R	R	F			R		R			R		R	R
A	16HCC	151.48	167.83	14.99	G	*	F	F		C	R					R	F	F				R		*				F	*	R	R	*		R		R			R		R	R
A	17H-2, 105-107	153.95	173.95	15.25	G	F	R	C		F	F		*			*	R	F		R		*		R				R	R	*	R	*		R		R					*	R
B	17HCC	155.64	174.92	15.32	G	R	R	C		F	R					R	R	F		*	*			R				R	R	R	R	*		R		R			*		R	R
A	17H-3, 149-150	155.89	175.89	15.38	G	*	F	C		F	R					R	*	F						R				F	*	R		R		*		R					R	R
A	17H-4, 105-107	156.95	176.95	15.45	M	F	F	C		C	R		*	*		R	*	F		*	R			*				F	R	R		*		R		R			R	R	R	R
A	17HCC	161.19	181.19	15.72	G		F	R		A	*			*		R	*	F		R	*			R	*			R	R	*		*		R		R			R	R	F	R
A	18H-2, 105-107	163.45	183.92	15.90	G		R	*		C	R					R	*	F		R	*			*	R			R	*	*		*		R		R			F	R	F	R
B	18HCC	164.78	185.08	15.97	G		R	*		C	R	*				R	*	F	R	R					R			R	*	*		F		R	*	R			F	R	F	R
A	18H-3, 149-150	165.39	185.86	16.02	G		F	*		A	R	*		*		*	*	F	R	*				*	R			R	R	*		R		R		R	R		R	R	F	R
A	18H-4, 105-107	166.45	186.92	16.09	G		F	*		A	R	R				*	*	F	*	R	*			R	R			R	R	R		F		*	R	R	R		R	F	F	*
A	18HCC	169.72	190.19	16.28	G		F	R		A	F	R		R		R	R	F	*		F			*	*			*	*	*		F		*		R	R		F	R	R	R
A	19H-2, 105-107	172.95	194.26	16.70	G		R	*		A	*	F		*		R		R		F	R			R	R							R			*	R	R		F	F	F	R
B	19HCC	174.81	197.12	16.90	G		R	*		A	*	F				R		F	*	R	R			*	R							R			*	R	R		F	F	F	R
A	19H-4, 105-107	175.95	197.26	16.91	G		R	*		C	*	R		*		*		F		R	*			*	*							R			*	R	*		F	F	C	*
A	19HCC	180.41	201.72	17.19	G			*		F	R	R				R		R	*	*	F			*	*							F			F	*	*		F	F	F	R
A	20H-2, 104-106	182.44	205.17	17.41	G			*		F	R	*				*		*	*	F				*	*							R				R	*		F	F	A	*
A	20H-4, 104-106	185.44	208.17	17.64	G			*		F	*	R		*				*	*	F				*								R				R	*		F	F	C	R
B	20HCC	184.35	208.38	17.66	G			*		C	*	R				*		*	*	F	*			*	*							R			*	R	*		F	F	C	*
A	20HCC	189.87	212.60	17.92	G			*		C	R	R						*	*	*	R				*							R			R	R	*		R	F	C	*
A	21H-1, 105-107	190.45	214.57	17.99	G			*		C	*	*		*		R		*	R	R	*				*										R	R	R		*	F	F	R
A	21H-3, 140-141	193.80	217.92	18.13	M			*		A	R	*		*		*		*	*	R					R										R	R	*		*	F	C	*
B	21HCC	193.42	218.47	18.16	G			*		C	R	*						*	R	F	*				R										R	R	*		R	F	C	R
A	21H-4, 105-107	194.95	219.07	18.19	G			*		F	*	*				R		*	R	F					R										R	*	*		F	F	F	R
A	21HCC	198.95	223.07	18.40	G			R		C	R	R						*	R	R	R				R										R	*	*		R	F	F	R
A	22H-2, 105-107	201.45	227.43	18.61	G			*		F	R	R				*		*	R	F					R											R	F		R	F	R	R
B	22HCC	202.81	228.78	18.67	G			*		F	R	R		*				*	R	F					R											R	F		R	F	F	R
A	22H-3, 140-141	203.30	229.28	18.70	G			*		F	R	R				*		*	R	R					R											R	F		F	F	F	*
A	22H-4, 105-107	204.45	230.43	18.75	G			*		F	*	F		*				*	R	R					*											*	F		F	F	F	*
A	22HCC	208.65	234.63	18.90	G			*		F	R	R				R		*	*	*	R				*										*	*	F		R	F	F	R

Appendix. *Continued 2.*

					No.	1	2	3	4	5	6	7	8	9	10	11	12	13	14	15	16	17	18	19	20	21	22	23	24	25	26	27	28	29	30	31	32	33	34	35	36	37
A	23H-2, 104-106	210.94	239.36	19.06	M			*		F	R	R				*			*	F						*									*	R	F		*	F	*	
B	23HCC	211.78	240.70	19.09	G			*		C	R	R		*					*	R	*				*	*									*	*	F		*	F	R	*
A	23H-3, 149-150	212.89	241.31	19.10	M			*		C	R	R		*		*			*	R			*		*	*									R	*	F		*	F	R	*
A	23H-4, 104-106	213.94	242.36	19.13	G			*		F		R		*		*				R																*	F		R	F		
A	23HCC	218.11	246.53	19.23	G			*		F	R	R		*		*			R	*	R		*			*										*	R		*	F		*
A	24H-2, 104-106	220.44	252.07	19.36	G			*		C	R	R							*	F	*		R			*									*	*	R		*	F		R
B	24HCC	222.11	253.20	19.38	G			*		F	R	R							*	R	*					*									R	*	F		*	F		
A	24H-3, 140-141	222.30	253.93	19.40	G			*		F	R	F		*		*			*	R			*			*									R	*	F		R	F		*
A	24H-4, 109-111	223.49	255.12	19.43	G			*		C	*	*							*	R	*		R			*									R	R	F		*	F		R
A	24HCC	227.84	259.47	19.53	G			F		F	R	*		*		R			*	*	F														*	R	F		*	F		
A	25H-2, 104-106	229.94	262.71	19.61	G			*		C	R	R				*			R	*	*		R			*	*										R		R	C		R
B	25HCC	231.42	263.96	19.64	G			*		F	R	R				*			*	R	*		R			*	*								R		F			F		*
A	25H-3, 149-150	231.89	264.66	19.66	G			*		F	R	R		*		*			*	R	*		*			*	*								F		F			F		R
A	25H-4, 104-106	232.94	265.71	19.68	G			R		F	R	R		*		*			*	*	*		*				*								R		F			F		R
A	25HCC	236.85	269.62	19.77	G			F	R	F	R	*		*		R			R	R	R					*	*								R		F			F		*